March 11, 1995

New Combined Track Bank

Keisuke Fujii

JLC Physics Group
KEK, Tsukuba 305, Japan

Abstract

A new track-cluster matching program is now available. The program is based on a new algorithm and produces new combined track banks. In this short note, we explain the philosophy of the new track-cluster matching program and show how to use it to improve mass resolution, etc. The performance of the program is demonstrated using some typical application examples.

The version presented here is a jlcux version of the original version on FACOM developed in May, 1993.

Chapter 1

Philosophy

1.1 overview

The goal of the cluster-track matching is to improve the momentum resolution of the detector system on the whole and consequently to identify, with the jet-invariant-mass method, partons such as W, Z, t, H, etc. Given the high performance of the JLC central tracker, the best performance is expected, when calorimetric information is only used for neutral particles. This requires the deletion of calorimetric clusters that match charged tracks detected in the central tracking device: notice that, when the energies of the charged tracks is subtracted, instead of deleted, from the energy deposites in the calorimeters, the energy fluctuations in the calorimetry remain in the measurements.

1.2 Algorithm

The new cluster-track matching program first identify electrons and muons with external particle-ID devices. Then EM-cluster-$e^{\pm}$-track matching is performed which is followed by HD-cluster-hadron-track matching. The cluster-track matching proceeds as follows. We first form global calorimetric clusters, which are contiguous calorimeter blocks with nonzero energy deposites (see Fig.1.1).

When such a global cluster contains no matched charged track, the cluster is recognized as a pure neutral particle and we assign a 4-momentum:

$$E^{N\mu} = (E^G, E^G \cdot \bar{\mathbf{x}}_G / \left|\bar{\mathbf{x}}_G\right|) \tag{1.2.1}$$

assuming it is a single massless neutral particle.

On the other hand, when the energy of the global cluster E^G is consistent with the energy of the corresponding charged tracks E^C:

$$E^G - E^C \leq n \cdot \sigma, \tag{1.2.2}$$

the global cluster is taken as consisting entirely of charged particles. We thus discard this global cluster and use only tracking information.

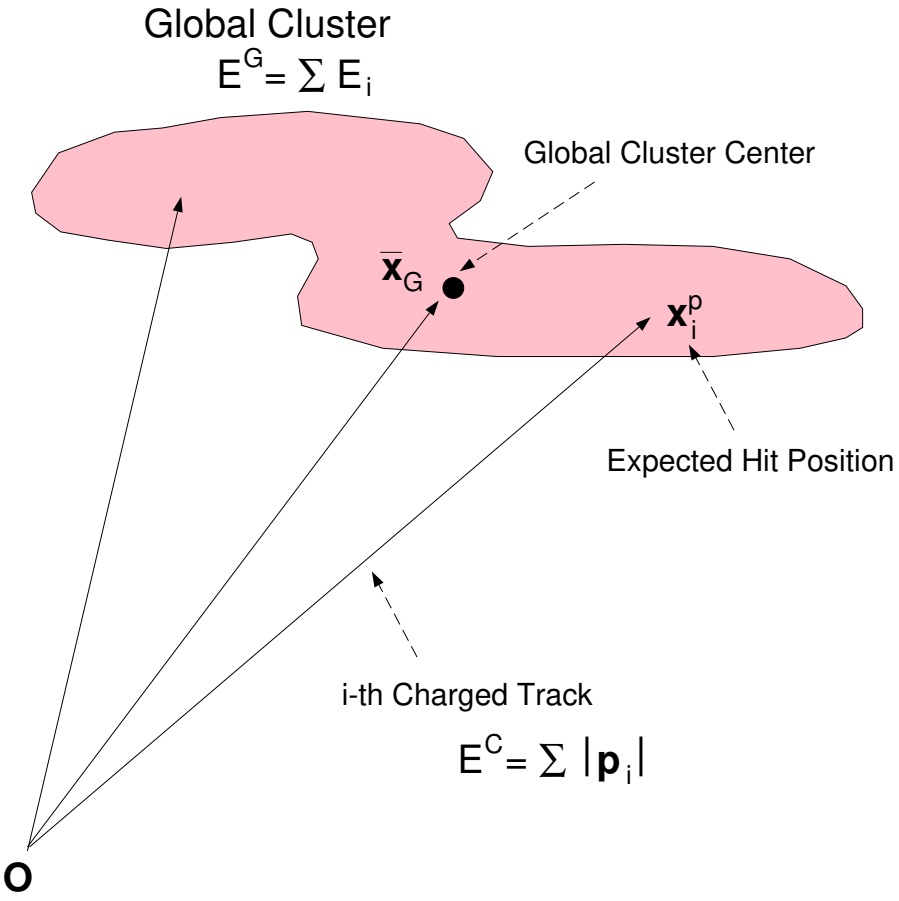

Figure 1.1: Global cluster and corresponding tracks

When the above matching condition is not satisfied:

$$E^G - E^C > n \cdot \sigma, \tag{1.2.3}$$

the global cluster is recognized as a mixed cluster consisting of both charged and neutral particles. In this case, we use all the charged tracks in this global cluster, while treating the energy difference as a single massless neutral particle with a 4-momentum:

$$E^{N\mu} = (E^N, \mathbf{E}^N), \tag{1.2.4}$$

where

$$\begin{aligned} E^N &= E^G - E^C \\ \mathbf{E}^N &= E^N \cdot \frac{E^G \bar{\mathbf{x}}_G - E^C \bar{\mathbf{x}}_C}{|E^G \bar{\mathbf{x}}_G - E^C \bar{\mathbf{x}}_C|} \\ &= E^N \cdot \frac{E^G \bar{\mathbf{x}}_G - \sum |\mathbf{p}_i| \mathbf{x}_i^p}{|E^G \bar{\mathbf{x}}_G - \sum |\mathbf{p}_i| \mathbf{x}_i^p|}. \end{aligned} \tag{1.2.5}$$

Chapter 2

Usage

2.1 Location of the Program

The new cluster-track matching program is in

```
/home/fujiik/work/a_ltkcl/lib/
```

where you can find both fortran source codes and a set of load modules prepared as a library:

```
/home/fujiik/work/a_ltkcl/lib/glib.a
```

2.2 Usage

You just need to call a subroutine

```
CALL CMBTRK(IRET)
```

then you get three new banks

```
Production:Combined_Gamma_Track
Production:Combined_Lepton_Track
Production:Combined_Hadron_Track.
```

Each element of these three banks corresponds to a particle entry which has the same format as follows:

```
RDATA(    1) = EX
     (    2) = EY
     (    3) = EZ
     (    4) = E
     (    5) = ECL if electrons, unused otherwise
     (    6) = EMC cluster # if electrons, unused otherwise
     (    9) = ICHG
```

```
(   10) = ITYP
(   11) = ISRC
(   12) = # used CDC tracks
(13-->) = CDC track serial number
```

where

```
ITYP =  1 : pure gamma
     =  2 : gamma in mixed EMC cluster
     =  3 : pure neutral hadron
     =  4 : hadron in mixed HDC cluster
     =  5 : pure charged hadron
     =  6 : unmatched track
     = 11 : electron candidate
     = 13 : muon candidate
ISRC = 100*IHDC + 10*IEMC + ICDC.
```

For instance 101 means the 4-vector was calculated from HDC and CDC information.

2.3 Important Notice

The $n \cdot \sigma$ cut used to delete clusters is heavily process-dependent and must be tuned for yourselves. The cut values can be different for electromagnetic and hadronic clusters and are stored in COMMON /CMBCUT/ as separate cut variables: ENSGEM for electromagnetic and ENSGHD for hadronic clusters. These cut values can be set by a block data:

```
      BLOCK DATA CMBBLK

      COMMON /CMBCUT/ ADXECT, ENSGEM, ENSGHD
      REAL*4          ADXECT, ENSGEM, ENSGHD

      DATA ADXECT /    20.0 /
C--
C  ENSGEM = n for EM-clusters
C--
      DATA ENSGEM /     2.0 /
C--
C  ENSGHD = n for HD-clusters
C--
      DATA ENSGHD /     2.0 /
      END
```

Chapter 3

Performance

3.1 W Mass Reconstruction

We have generated W bosons isotropically in the momentum range

$$0 \leq P_W \leq 500\text{GeV}$$

with $\Gamma_W = 0$. The generated events are passed through the JLC-standard-detector simulation and the invariant mass of the final state particles is calculated for each event without any selection cuts. Fig.3.1 compares the invariant mass distribution for calorimetric information only and that after the new cluster-track matching.

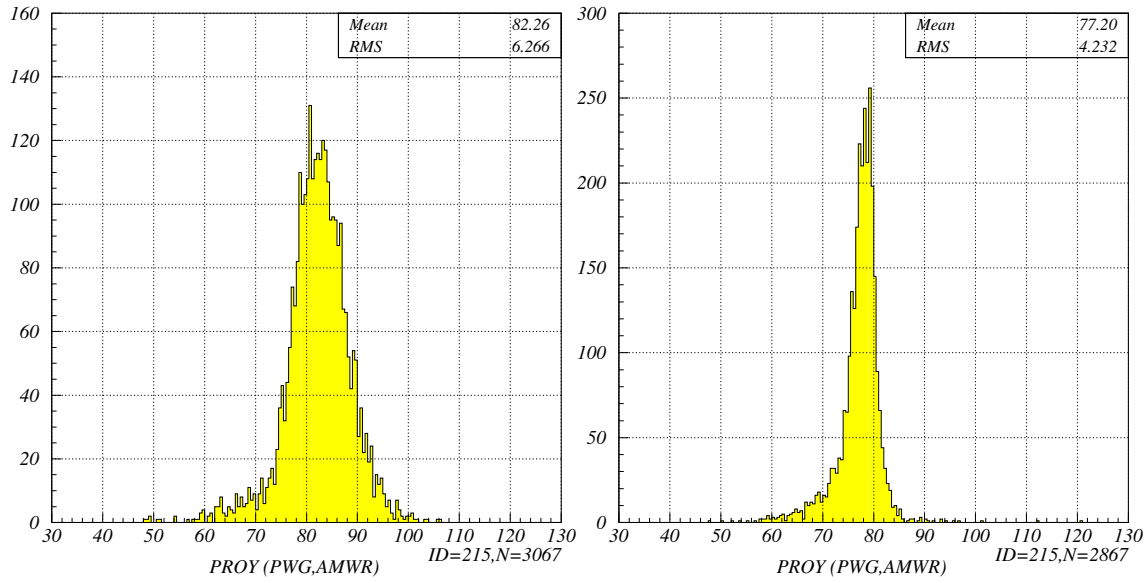

Figure 3.1: Reconstructed W mass distributions for (left) calorimetric information only and (right) combined track information. In the cluster-track matching 2-σ cut is used to delete global clusters.

Fig.3.2 corresponds to blown-up of Fig.3.1, again (left) for calorimetric information only and (right) for combined track information. The figure tells us that, after the new

cluster-track matching we have

$$< \Delta M_W > \simeq -1.5\text{GeV},$$

not too good showing the 2-σ cut is to much, while the mass resolution improves to

$$\sigma_W \simeq 1.8\text{GeV},$$

which is quite good compared to the mass resolution in excess of 4GeV with the calorimetric information only.

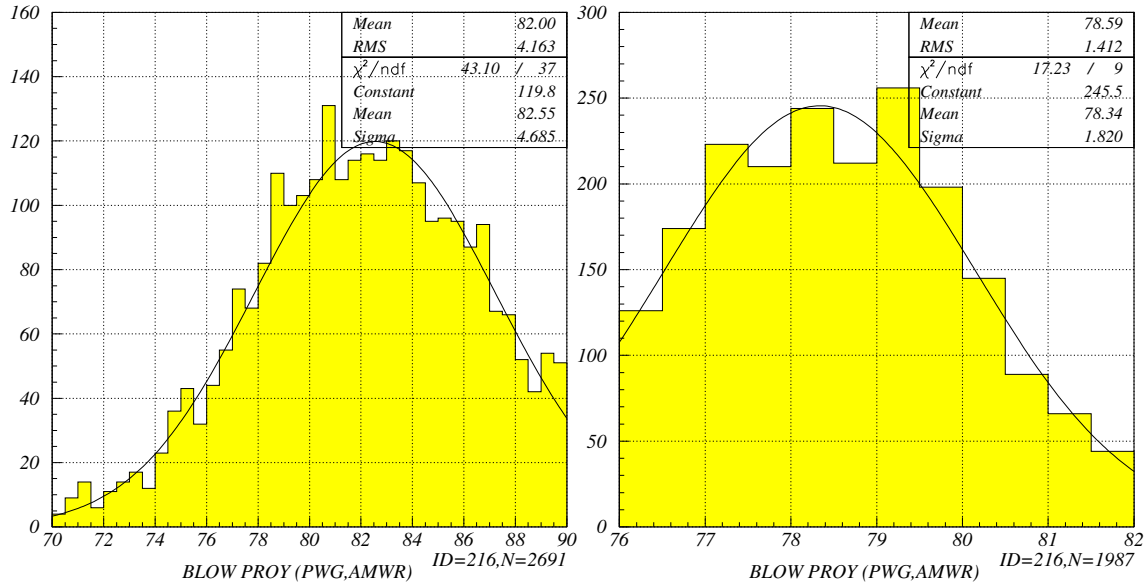

Figure 3.2: Blown-up figure of Fig.3.1, where the smooth curves are the result of Gaussian-fits: (left) calorimetric information only and (right) combined track information.

When we examine the mass distribution as a function of momentum, we get Fig.3.3.

We can see that both the resolution and the center value are momentum-dependent even after the new cluster-track matching: $\sigma_W \simeq 1.6$GeV at best, while the center value decreases with momentum, showing that the rate of cluster misdeletions goes up with momentum. The mass resolution and the systematic shift of the center value depend on the choice of the $n \cdot \sigma$ cut.

3.2 Higgs Mass Reconstruction

In order to see the effects of the choice of the $n \cdot \sigma$ cut, we have studied Higgs production in $e^+e^- \to HZ$ and $Z \to \nu\bar{\nu}$. Figs.3.4-a) to -c) plot reconstructed Higgs mass distributions with three different values of $n \cdot \sigma$ cut: 1.0-σ, 1.5-σ, and 2.0-σ. These three figures should be compared to each other as well as to Fig.3.4-d) which is the mass distribution with smeared generated tracks. We can see that when n is too small, we have a upward tail

in the distribution because of undeleted clusters due to charged hadrons. On the other hand, a too large n misdeletes clusters due to neutral hadrons and consequently lowers the center value of the mass peak.

3.3 Top Momentum Reconstruction

Another interesting example is the top momentum reconstruction. We compare in what follows the reconstructed top momentum distribution with calorimetric information only and that with the new combined track information for $e^+e^- \to t\bar{t} \to$ lepton + 4 jets with $m_t = 150\text{GeV}$ and $\sqrt{s} = 300\text{GeV}$.

Fig.3.5 compares the residual distributions of top momentum reconstruction with only calorimetric (left) and combined track information (right).

When projected to the vertical axis, the difference becomes clear (see Fig.3.6).

We can see a significant improvement of momentum resolution. It should also be noted that the systematic shift of the center value also gets smaller when the combined track information is used as seen in Fig.3.7

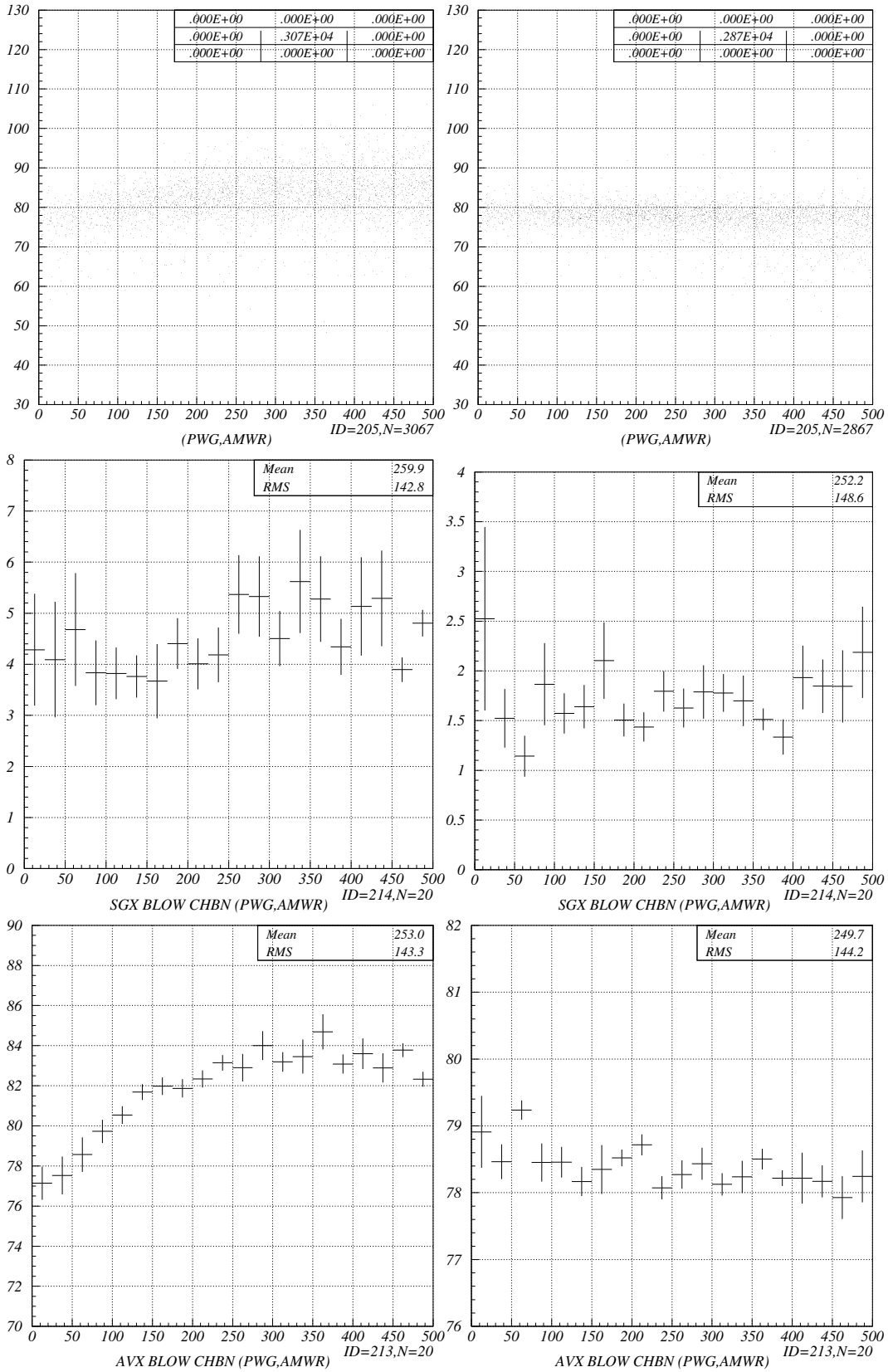

Figure 3.3: Reconstructed W mass plotted against W momentum and its standard deviation and center value as functions of the W momentum: (left) calorimetric information only and (right) combined track information.

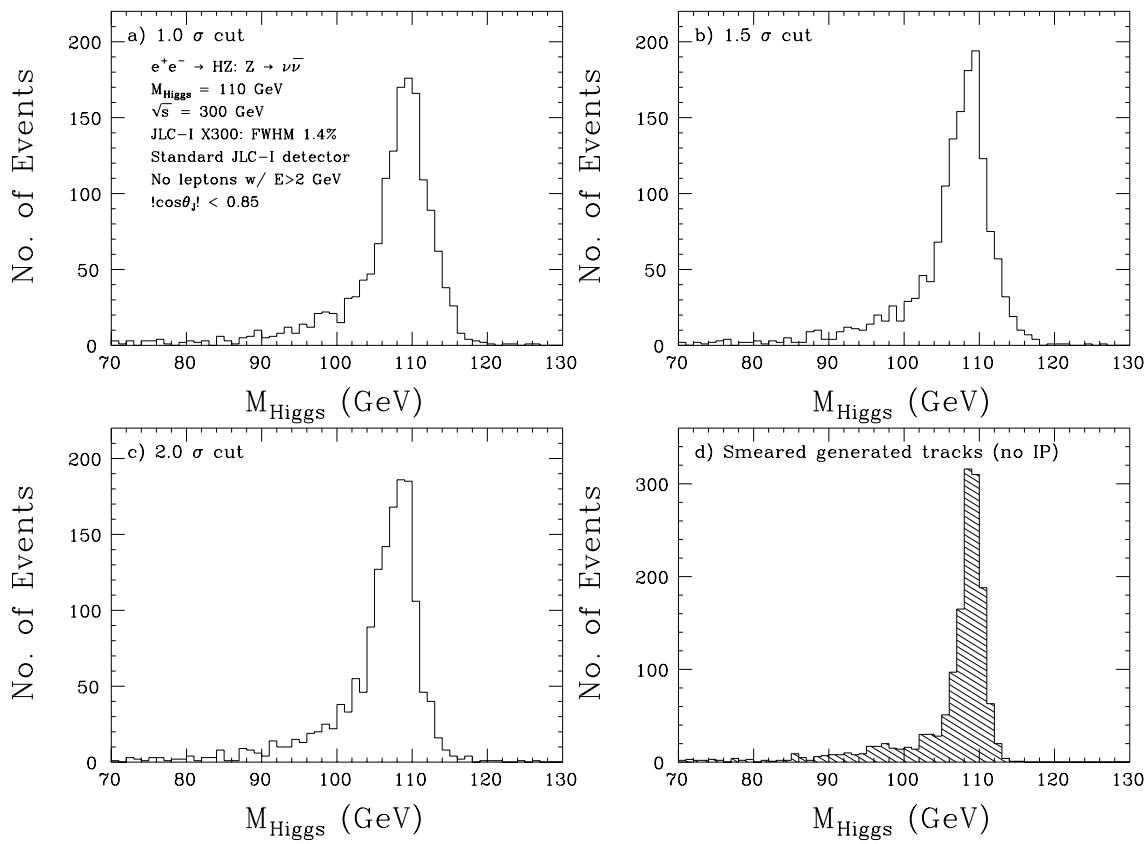

Figure 3.4: Reconstructed Higgs mass distributions with different $n \cdot \sigma$ cuts: (a) 1.0-σ, (b) 1.5-σ, and (c) 2.0-σ. (d) is that for smeared generated tracks.

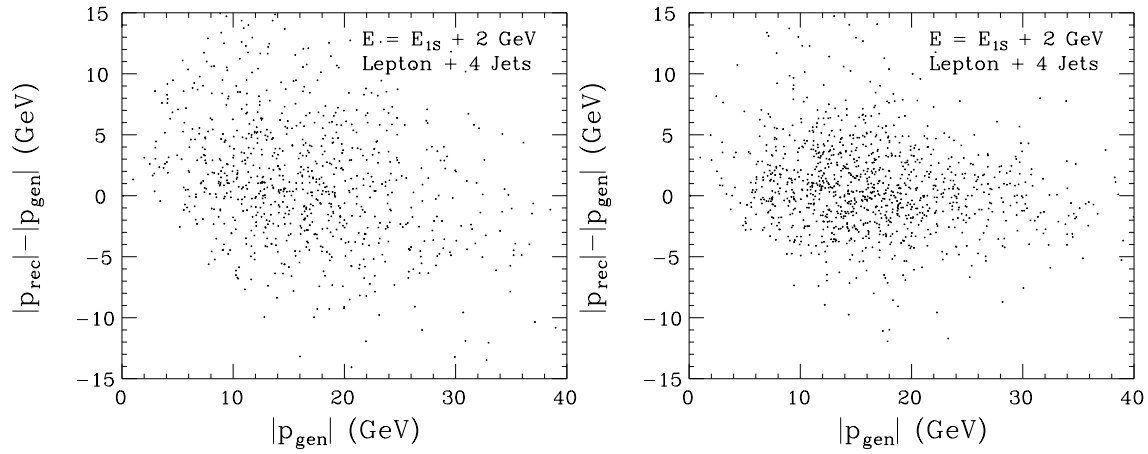

Figure 3.5: Difference of reconstructed and generated top momenta plotted against generated top momentum: (left) calorimeter only and (right) combined track information.

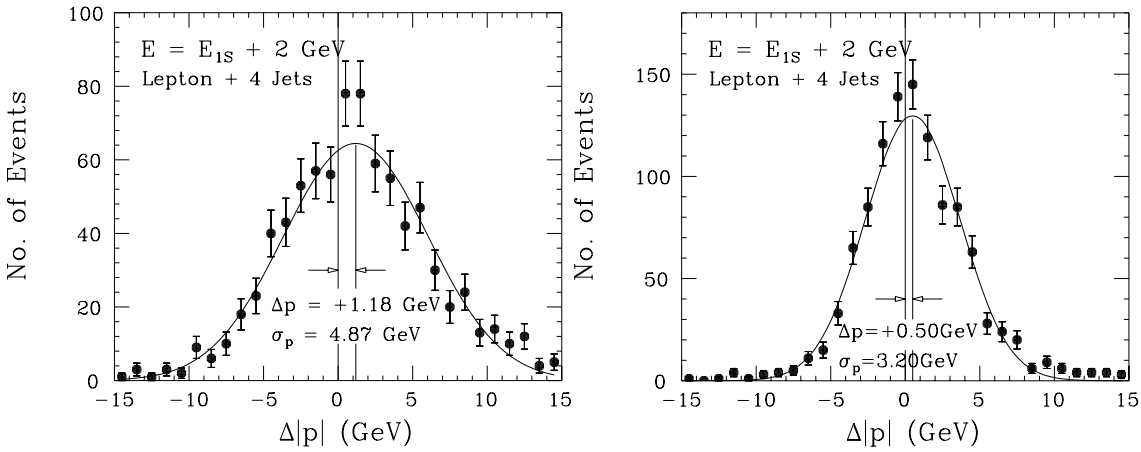

Figure 3.6: Projections to the vertical axis of Fig.3.5: (left) calorimeter only and (right) combined track information.

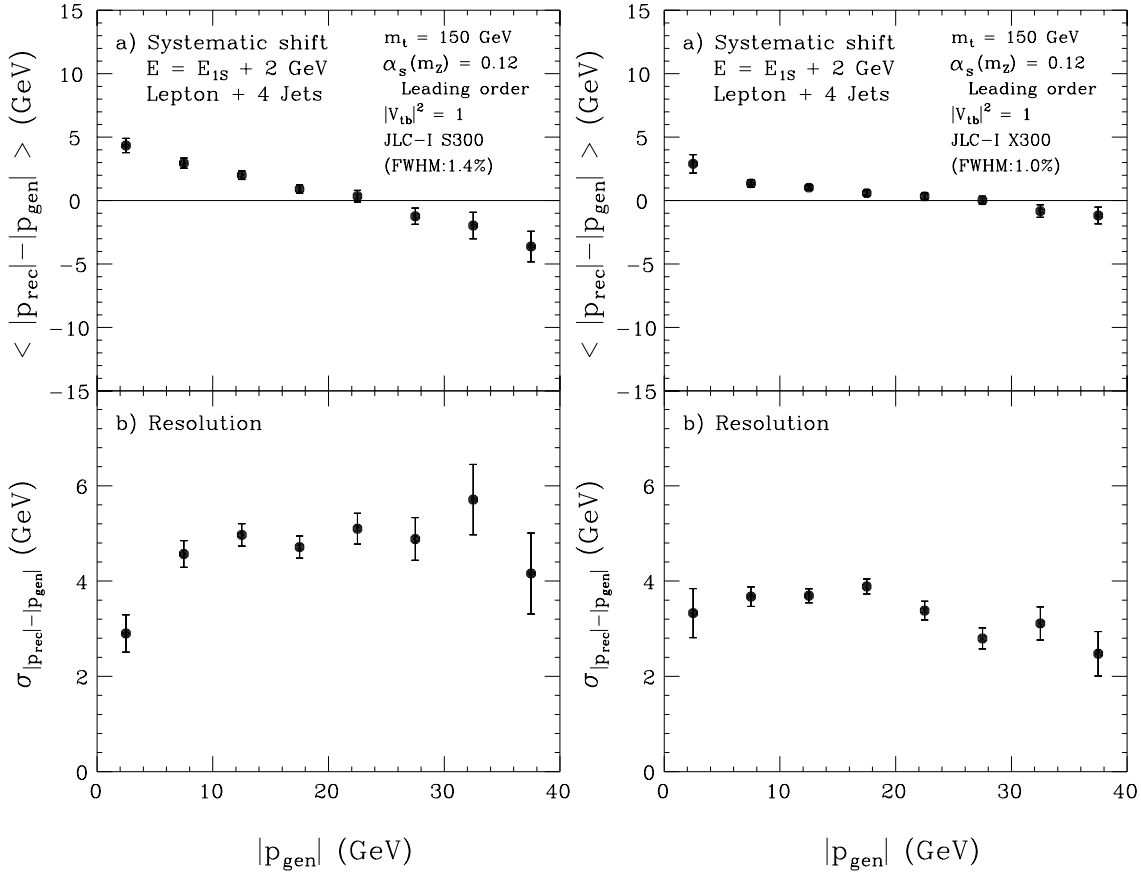

Figure 3.7: Average and standard deviation of Fig.3.5 for each momentum bin plotted as a function of top momentum: (left) calorimeter only and (right) combined track information.

Chapter 4

Summary

We have developed a new cluster-track matching program. This program improves the invariant mass resolution for W and Higgs mass reconstructions, when the $n \cdot \sigma$ cut is appropriately chosen. The W mass resolution so obtained is around 1.6GeV which is now pretty close to $\Gamma_W/2$.

A significant improvement is also achieved in top momentum reconstruction. This benefits us by providing highter detection efficiency, better momentum resolution, and smaller systematic shift in the center value of the reconstructed top momentum.